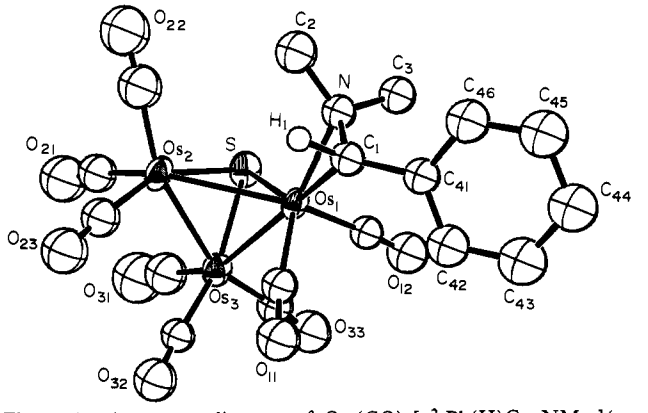

Figure 1. An ORTEP diagram of $Os_3(CO)_8[\eta^2\text{-Ph(H)C=NMe}_2](\mu_3\text{-S})(\mu\text{-H})$, **2**, showing 50% probability thermal ellipsoids.

Scheme I

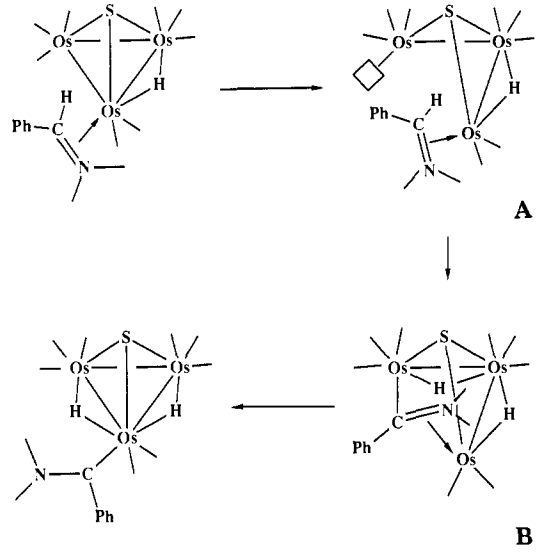

site on an adjacent metal atom. Since CO loss was not observed in the transformation, an alternative mode of vacant site formation has been considered. This involves a metal–metal bond cleavage to form an intermediate A as shown in Scheme I. C–H bond cleavage in the iminium ligand would lead to a bridging (η^2-dimethylamino)carbene ligand,[13] B, analogous to a σ–π alkenyl ligand, eq 2. A closing of the cluster would lead to the conversion of the bridging carbene into a terminal carbene. We have recently observed a similar transformation of a (μ_3-η^2-dimethylamino)-carbene ligand into a terminal carbene ligand.[14]

In our recent studies we have discovered several examples of the transformation of tertiary amines into aminocarbene ligands in metal clusters by C–H activation processes. These results provide the first evidence concerning the way in which iminium ligands might be involved in these processes.[9,15]

Acknowledgment. These studies were supported by the Office of Basic Energy Science of the U.S. Department of Energy. We thank Johnson Matthey Inc. for a loan of osmium tetroxide. NMR measurements were made on a Brüker AM-300 spectrometer purchased with funds from the National Science Foundation under Grant no. CHE-8411172.

Supplementary Material Available: Tables of crystallographic data, fractional atomic coordinates and thermal parameters, selected interatomic distances and angles, and anisotropic thermal parameters (7 pages); table of structure factor amplitudes (17 pages). Ordering information is given on any current masthead page.

(13) Davis, J. H., Jr.; Lukehart, C. M.; Sacksteder, L. *Organometallics* **1987**, *6*, 50.
(14) Adams, R. D.; Babin, J. E. *Organometallics* **1987**, *6*, 1364.
(15) (a) Adams, R. D.; Kim, H. S.; Wang, S. *J. Am. Chem. Soc.* **1985**, *107*, 6107. (b) Adams, R. D.; Babin, J. E.; Kim, H. S. *Inorg. Chem.* **1986**, *25*, 4319.

The Influence of Surface Atomic Steps on Site-Selective Adsorption Processes. Ethylidyne Formation on Rh{111} and Rh{331}

Robert Levis and Nicholas Winograd*

The Pennsylvania State University
Department of Chemistry, 152 Davey Laboratory
University Park, Pennsylvania 16802

Lisa A. DeLouise

Xerox Corporation, M/S 114-41D
Webster, New York 14580

Received May 26, 1987

Crystal defects such as steps and kinks are considered to be active sites which enhance molecular bond-breaking events in heterogeneous catalytic reactions.[1] In this communication, we present new evidence that suggests that for a class of site-specific reactions, these defects may actually inhibit the desired reaction pathway. Our conclusions are based on studies of CO and C_2H_4 adsorption on Rh{111} and Rh{331} single crystal surfaces at room temperature. These model systems are of interest for several reasons. The Rh{111} surface as depicted at Figure 1a possesses an array of three-fold sites so as to accommodate the observed c(4 × 2) low energy electron diffraction (LEED)[2] structure for ethylidyne. The Rh{331} surface, however, is characterized by three rows of a {111} terrace and a {111} single atomic step as shown in Figure 1b. This structure contains only 80% of the number of three-fold sites that are present on Rh{111}. Ethylene undergoes dehydrogenation to CCH_3 (ethylidyne) and presumably requires a three-fold symmetric anchoring position.[3] Carbon monoxide, on the other hand, has been observed to bond to a plethora of binding sites, the nature of which are coverage dependent.[2,4,5] By simultaneously dosing both surfaces with equal amounts of CO or C_2H_4, we show with use of X-ray photoelectron spectroscopy (XPS) that the coverage of CO on the two crystal surfaces is identical, while the ethylidyne coverage on Rh{331} scales precisely with the number of available active sites. The results suggest that these step defects may then inhibit certain structure-sensitive reactions and that ethylidyne itself may be a novel titrant to determine the number of these sites on polycrystalline surfaces.[6]

Experiments were performed with use of a multitechnique surface analysis system described earlier.[7] Both the {111} and {331} crystals were affixed to the same sample manipulator and cleaned by using previously developed procedures until no impurity peaks could be observed by XPS. The crystals were then annealed at 1300 K until the characteristic LEED diffraction pattern was observed at room temperature and were subsequently dosed at 300 K with 10 langmuirs[6] of Matheson Research grade CO or C_2H_4 (at 10^{-7} Torr for 100 s). The C ls and O ls peak areas were determined by subtracting the background Rh signal. The pho-

(1) Davis, S. M.; Zaera, F.; Somorjai, G. A. *J. Am. Chem. Soc.* **1982**, *104*, 7453.
(2) Castner, D. G.; Sexton, B. A.; Somorjai, G. A. *Surf. Sci.* **1978**, *71*, 519.
(3) Skinner, P.; Howard, M. L.; Oxton, I. A.; Kettle, S. F. A.; Powell, D. B.; Sheppard, N. *J. Chem. Soc., Faraday Trans. 2* **1981**, *77*, 1203.
(4) Dubois, L. H.; Somorjai, G. A. *Surf. Sci.* **1980**, *91*, 514.
(5) DeLouise, L. A.; White, E. J.; Winograd, N. *Surf. Sci.* **1984**, *147*, 252.
(6) Beebe, T. P.; Yates, J. T. *Surf. Sci.* **1986**, *173*, L606.
(7) DeLouise, L. A.; Winograd, N. *Surf. Sci.* **1984**, *138*, 417.

0002-7863/87/1509-6873$01.50/0

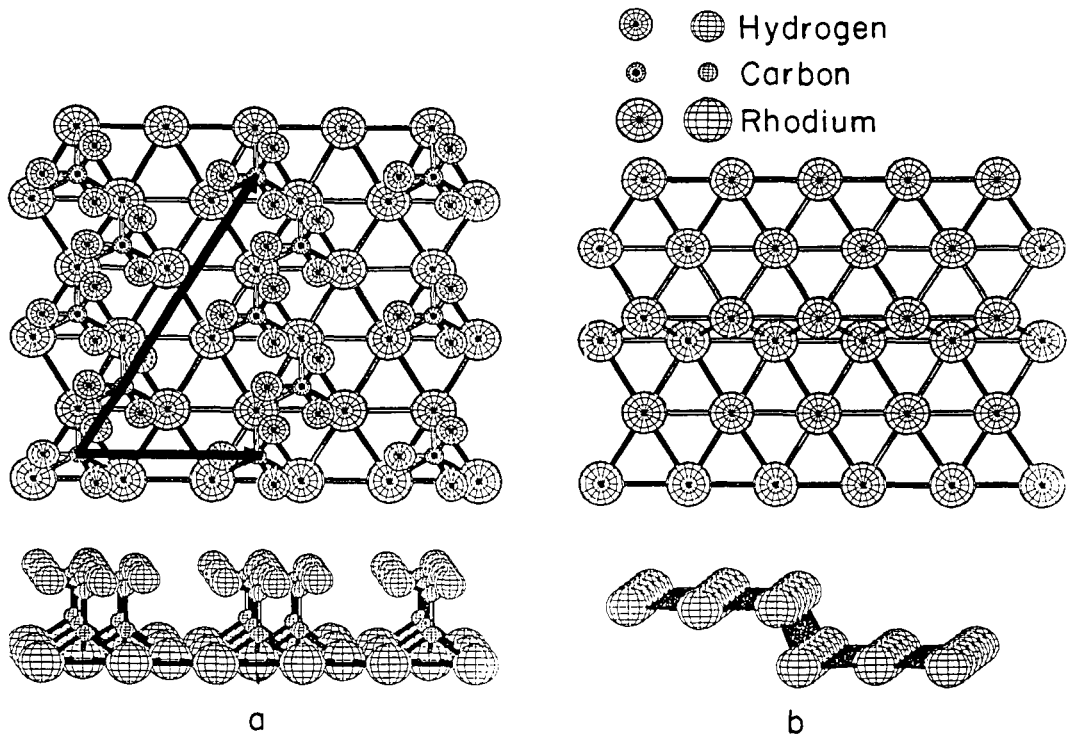

Figure 1. Schematic diagram of Rh{111} and Rh{331}. The Rh{111} surface with alternating rows of ethylidyne is shown in (a). The c(4 × 2) real space lattice vectors are shown. Note: The van der Waals radii for C and Rh are reduced for clarity. The Rh{331} surface with the three-row {111} terrace and the {111} step is illustrated in (b).

toelectron take-off angle was kept at 35° as measured from the plane of the surface to avoid focusing effects. In addition, the acceptance aperture was widened to integrate possible angular anisotropies in the electron yield. All XPS binding energies (BE's) are reported with respect to the Rh Fermi energy which places the Rh $3d_{5/2}$ peak at 307.1 eV.

Reproducibility of XPS peak area measurements was established by examining CO chemisorption on the two crystal surfaces and to provide a C coverage reference for the ethylidyne studies. As shown in Figure 2a,b both surfaces yield similar XPS spectra exhibiting a C ls BE of 285.9 eV. Previous XPS studies of the O ls line shape suggest that similar amounts of linear and bridge sites are observed on both surfaces under these conditions.[5] The saturation coverage is therefore determined more by interactions between CO molecules than by the number of available surface bonding sites.

After exposure of the clean surfaces to 10 L of ethylene at room temperature, a dramatically different picture emerges from analysis of the XPS spectra. Under similar conditions, both electron energy loss spectroscopy (EELS)[8] and LEED[9] experiments on Rh{111} suggest the dominant surface species is ethylidyne. The XPS C ls BE of 284.1 eV is certainly consistent with this assignment, altough we could not rule out the possibility of carbide formation as its C ls BE appears at 283.8 eV.[10] Thermal stability experiments performed by recording XPS spectra between 298 and 800 K suggest there is a similar reaction pathway for ethylene adsorption on Rh{331}.[11]

There are two crucial pieces of information contained in the C ls intensity measurements given in Figure 2. First, for Rh{111}, the integrated peak area shows that the c(4 × 2) overlayer structure exhibits a coverage of 94% of that found for CO after correcting for the fact that ethylidyne contains 2 C atoms. The CO coverage has been determined to be 0.62 monolayer (ML)

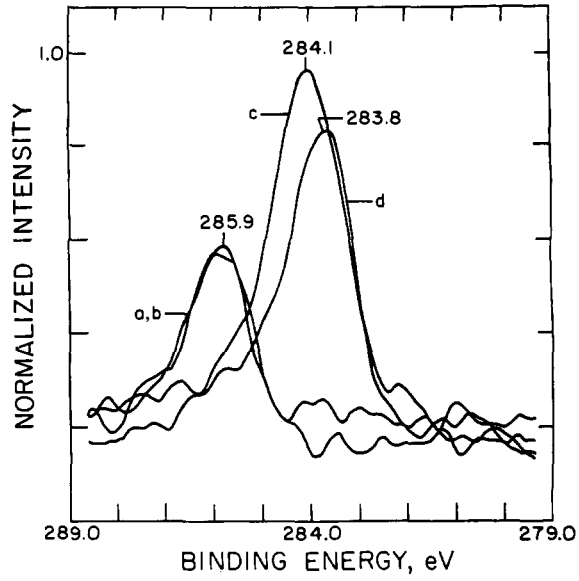

Figure 2. Carbon 1s photoelectron spectra for (a,b) a 10-L exposure of CO on the Rh{111} and Rh{331} surfaces at 300 K, (c) a 10-L exposure of C_2H_4 on the Rh{111} surface at 300 K, and (d) a 10-L exposure of C_2H_4 on the Rh{331} surface at 300 K. The Rh $3d_{5/2}$ peak areas are equivalent to within 97% of each other for the two crystal faces.[10]

from LEED, EELS, and thermal desorption experiments[2,12] implying that the ethylidyne coverage is 0.58 mL. The conventional c(4 × 2) LEED structure implies a coverage of 0.25 mL. Note that an anomalously high carbon coverage has been previously reported on Pt{111}.[13] Shown in Figure 1 is our proposed structure which would also yield a c(4 × 2) pattern. This unique alternating row configuration, with sterically locked hydrogen atoms, corresponds to 0.5 mL coverage and appears to be a highly stabilized geometry. The second important feature is that the C ls integrated

(8) Dubois, L. H.; Castner, D. G.; Somorjai, G. A. *J. Chem. Phys.* **1980**, *72*(9) 5234.
(9) Koestner, R. J.; Van Hove, M. A.; Somorjai, G. A. *Surf. Sci.* **1982**, *121*, 321.
(10) Levis, R. J.; Winograd, N., in preparation.
(11) Levis, R. J.; DeLouise, L. A.; White, E. J.; Winograd, N., in preparation.
(12) Dubois, L. H.; Somaridi, G. A. *Surf. Sci.* **1980**, *91*, S14.
(13) Yo, R.; Gusafsson, T. *Surf. Sci.* **1987**, *182*, L234. Freyer, N.; Pirug, G.; Bonzel, H. P. *Surf. Sci.* **1983**, *125*, 327.

intensity for Rh{331} is reduced to 79 ± 2% of that found for Rh{111}. The LEED I-V[9] calculations and EELS[8] measurements suggest that ethylidyne binds to three-fold sites on the {111} plane. The observed decrease in C ls intensity on Rh{331} scales precisely as the decrease in the number of three-fold holes available for binding. Note from Figure 2 that the presence of the step removes 20%[14] of these sites. Although it is not yet possible to identify the overlayer structure on Rh{331}, we note that it is possible to construct the same zig-zag geometry postulated for Rh{111} without steric interference from the step itself.

In summary, we have performed accurate carbon coverage measurements for CO and C_2H_4 adsorption on Rh{111} and Rh{331}. The results suggest that a very stable structure with interlocking hydrogen atoms is formed on the {111} plane and that the presence of the step on the {331} surface inhibits ethylidyne formation by reducing the number of active sites. It is of interest that the high site specificity of this reaction may provide a selective titrant for threefold sites on polycrystalline surfaces.

Acknowledgment. We are grateful to David Deaven for his assistance with computer graphics. We acknowledge the financial support of the National Science Foundation, the Air Force Office of Scientific Research, and the Office of Naval Research.

(14) The surface atom density ratio for Rh{331}/Rh{111} is 1.2, including step atoms (or step sites). Removing the step atoms (or step sites), covering $^1/_3$ of the Rh{331} surface leaves a ratio of 0.80 or 80%.

Unprecedented Bonding of a Coordinated Polyenyl Ligand. Synthesis and Molecular Structures of *fac*-Trialkyltricarbonyliron Compounds Containing the η^3-Nonafluorocycloocta-2,5-diene-1,4,7-triyl Ligand and Its Derivatives

Richard T. Carl,[1a] Russell P. Hughes,*[1a]
Jocelyn A. Johnson,[1a] Raymond E. Davis,*[1b] and
Ram P. Kashyap[1b]

Chemistry Departments, Dartmouth College
Hanover, New Hampshire 03755
University of Texas at Austin
Austin, Texas 78712

Received June 19, 1987

While hydrocarbon enyl and polyenyl ligands are ubiquitous in organotransition metal chemistry, (η^3-pentafluoroallyl)tricarbonylcobalt **1**[2] and the (η^3-nonafluorocyclohexenyl)tricarbonyliron anion **2**[3] appear to be the only reported examples

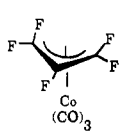

1

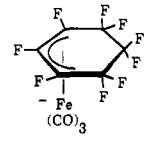

2

of complexes containing perfluorinated enyl ligands. No compounds containing perfluoropolyenyl ligands have been reported. We now report that the perfluorocycloocta-2,5-diene-1,4,7-triyl ligand and its derivatives can be prepared by nucleophilic attack on coordinated octafluorocyclooctatetraene. These perfluoropolyenyl ligands bind to the metal via three σ-bonds rather than through the π-system of the polyenyl ring, affording the first examples of trialkyltricarbonylmetal complexes.

(1) (a) Dartmouth College. (b) University of Texas at Austin.
(2) Stanley, K.; McBride, D. W. *J. Organomet. Chem.* **1975**, *53*, 2537-2541.
(3) Parshall, G. W.; Wilkinson, G. *J. Chem. Soc.* **1962**, 1132-1134.

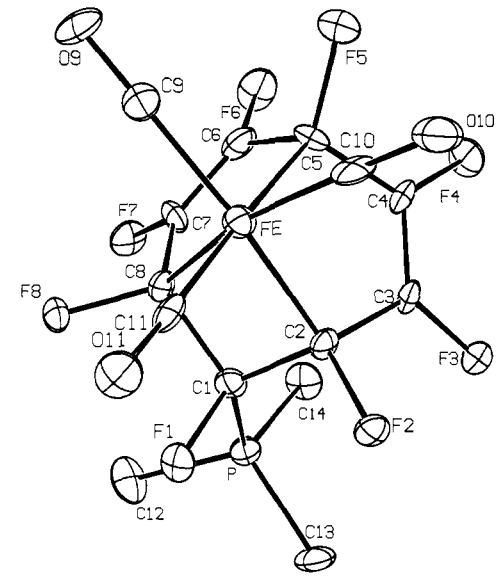

Figure 1. ORTEP drawing and numbering scheme for **6**. Selected bond distances (Å) and bond angles (deg) are as follows: Fe-C(2), 2.006 (8); Fe-C(5), 2.058 (11); Fe-C(8), 2.013 (8); Fe-C(9), 1.833 (9); Fe-C(10), 1.821 (8); Fe-C(11), 1.797 (11); P-C(1), 1.854 (9); P-C(12), 1.810 (10); P-C(13), 1.788 (8); P-C(14), 1.784 (13); C(1)-C(2), 1.519 (11); C(1)-C(8), 1.536 (10); C(2)-C(3), 1.487 (14); C(3)-C(4), 1.324 (12); C(4)-C(5), 1.448 (12); C(5)-C(6), 1.475 (10); C(6)-C(7), 1.315 (14); C(7)-C(8), 1.465 (13); C(9)-O(9), 1.129 (10); C(10)-O(10), 1.139 (11); C(11)-O(11), 1.1709 (13); C(2)-Fe-C(5), 83.8 (4); C(5)-Fe-C(8), 83.3 (4); C(8)-Fe-C(9), 94.7 (3); C(9)-Fe-C(10), 98.3 (4); C(10)-Fe-C(11), 94.8 (5); C(11)-Fe-C(2), 92.3 (4).

We have shown previously that the Co and Rh complexes **3**[4] undergo thermal reaction with *t*-BuNC or PMe_3 at the metal center, affording the octafluorocycloocta-2,5,7-triene-1,4-diyl complexes **4**[5] as the initial products. In contrast, reaction of the

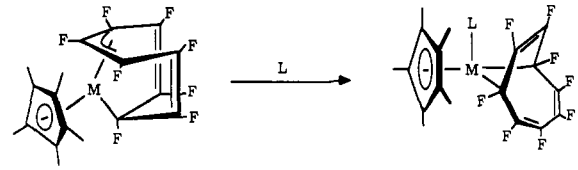

3 M = Co, Rh

4 M = Co, Rh
L = t-BuNC, PMe_3

corresponding iron complex **5**[6] with PMe_3 yielded white crystals of a 1:1 adduct **6**.[7] Retention of the $Fe(CO)_3$ moiety was confirmed by the IR spectrum, and the ^{19}F NMR spectrum exhibited five resonances of relative intensity 2:2:1:1:2, indicating retention

(4) Carl, R. T.; Doig, S. J.; Geiger, W. E.; Hemond, R. C.; Hughes, R. P.; Kelly, R. S.; Samkoff, D. E. *Organometallics* **1987**, *6*, 611-616.
(5) Hughes, R. P.; Carl, R. T.; Hemond, R. C.; Samkoff, D. E.; Rheingold, A. L. *J. Chem. Soc., Chem. Commun.* **1986**, 306-308.
(6) Barefoot, A. C., III; Corcoran, E. W., Jr.; Hughes, R. P.; Lemal, D. M.; Saunders, W. D.; Laird, B. B.; Davis, R. E. *J. Am. Chem. Soc.* **1981**, *103*, 970.
(7) **6**: 44%; mp 144-146 °C dec; IR (CH_2Cl_2) ν_{CO} 2100, 2080, 2005, $\nu_{C=C}$ 1717 cm^{-1}; ^{19}F NMR ($CDCl_3$, shifts upfield from internal $CFCl_3$, see drawing for numbering) δ 113.9 (m, F_4), 126.6 (m, F_3), 155.5 (m, F_1, J_{P-F} = 138 Hz), 176.4 (m, F_5), 187.8 (m, F_2); ^1H NMR ($CDCl_3$) δ 1.86 (d, J_{P-H} = 14 Hz, PMe_3); ^{31}P NMR ($CDCl_3$, shifts upfield from external H_3PO_4) δ 17.7, d, J_{P-F} = 138 Hz). Calcd for $C_{14}H_9F_8FeO_3P$: C, 36.24; H, 1.95. Found: C, 36.12; H, 1.78. Crystal data: orthorhombic, $P2_1/c$, a = 13.652 (3) Å, b = 10.228 (2) Å, c = 13.132 (5) Å, β = 116.65 (2)°, Z = 4. The structure solved by heavy atom methods and refined by full-matrix least-squares procedures to final agreement factors $R = \sum(||F_o| - |F_c||)/\sum|F_o| = 0.0755$, $R_w = [\sum w(|F_o| - |F_c|)^2/\sum w|F_o|^2]^{1/2} = 0.0740$, by using 2401 reflections with $F_o \geq 4.0\ \sigma(F_o)$. X-ray experimental procedures, data processing, and principal computer programs were essentially as described previously by Riley and Davis (Riley, P. E.; Davis, R. *Acta Crystallogr., Sect B: Struct. Crystallogr.* **1976**, *B32*, 381-386). Full details are provided as Supplementary Material (see paragraph at end of text).

0002-7863/87/1509-6875$01.50/0